

Triple Michelson Interferometer for a Third-Generation Gravitational Wave Detector

A Freise, S Chelkowski, S Hild, W Del Pozzo, A Perreca
and A Vecchio

School of Physics and Astronomy, University of Birmingham, Edgbaston,
Birmingham B15 2TT, UK

E-mail: adf@star.sr.bham.ac.uk

Abstract. The upcoming European design study ‘Einstein gravitational-wave Telescope’ represents the first step towards a substantial, international effort for the design of a third-generation interferometric gravitational wave detector. It is generally believed that third-generation instruments might not be installed into existing infrastructures but will provoke a new search for optimal detector sites. Consequently, the detector design could be subject to fewer constraints than the on-going design of the second generation instruments. In particular, it will be prudent to investigate alternatives to the traditional L-shaped Michelson interferometer. In this article, we review an old proposal to use three Michelson interferometers in a triangular configuration. We use this example of a triple Michelson interferometer to clarify the terminology and will put this idea into the context of more recent research on interferometer technologies. Furthermore the benefits of a triangular detector will be used to motivate this design as a good starting point for a more detailed research effort towards a third-generation gravitational wave detector.

PACS numbers: 04.80.Nn, 07.60.Ly, 95.75.Kk, 95.55.Ym

1. Introduction

The first generation of large-scale laser-interferometric gravitational-wave detectors, consisting of GEO 600 [1], Virgo [2], LIGO [3] and TAMA300 [4] is now in operation and collects data of unprecedented sensitivity and bandwidth. All of these detectors have successfully performed long-duration data recording runs. The path for the second generation of laser-interferometric detectors is clearly laid out: strong R&D projects are currently being carried out for Advanced LIGO [5], Advanced Virgo [6], LCGT [7] and GEO-HF [8], of which all except the LCGT project are planned as advanced technology upgrades of the existing detectors.

However, these second generation detectors are expected to approach the sensitivity limits given by the current infrastructures. The use of new detector sites can be an interesting alternative. Such sites, especially if underground, could not only allow third-generation detectors to improve the sensitivity by a factor of ten in a wide frequency range but would be an investment providing enough scope for future upgrades of the instrument over a substantial period of time. In Europe a broad collaboration, including the GEO and Virgo groups has begun a design study for a third-generation gravitational-wave detector called ‘Einstein gravitational-wave Telescope’ (ET) [9, 10]. This project aims at building an instrument that provides a

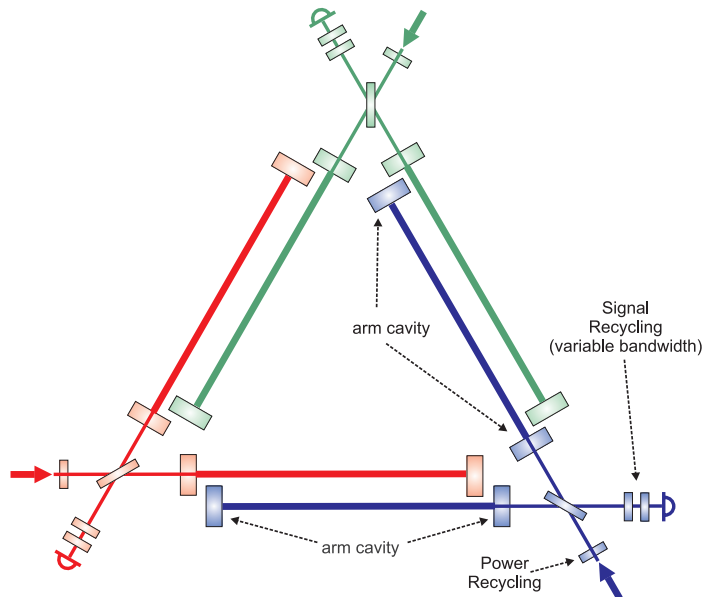


Figure 1. Example optical layout of an interferometric gravitational-wave detector with a triangular geometry. The sketch shows a detector formed by three coplanar interferometers that form an equilateral triangle. The interferometers are based on the Michelson topology. However, the interferometer configuration includes additional optical technologies, like resonant arm cavities, power recycling, and a tunable cavity as a signal recycling mirror. Further information about the detailed detector configuration would be provided by the parameters of the optical elements and the operating point of the mirror position control system. This example shows how three state-of-the-art interferometers could be combined to a new type of detector.

strain sensitivity about a hundred times better than first generation detectors¹ and to shift the lower end of the observational window to frequencies of approximately 1 Hz [11].

This article introduces some useful concepts and methods for the classification of possible designs of third-generation detectors. In Section 2 we discuss the concepts of detector *geometry*, *topology* and *configuration*. In the following Sections we review aspects of triangular detector topologies which, to some extent, have been discussed within the context of the space-borne detector LISA [12]. We recall an early proposal of a ground-based, triangular set of co-located Michelson interferometers originally suggested by Rüdiger, Winkler and collaborators [13, 14] and provide further arguments for this geometry and topology. While this design represents only one of many possibilities for future detectors, it features the best understood long-baseline interferometer, the Michelson interferometer, yet offers interesting opportunities for *virtual interferometry* (see Section 3). In particular, it allows the construction of a simple *null-stream* (see Section 4), while being cost-effective to build (see Section 6). We conclude in Section 7 with a summary and outlook.

¹ This is equivalent to a strain sensitivity ten times better than those planned for second-generation detectors.

2. Detector Geometry, Topology and Configuration

The terms geometry, topology and configuration are often used loosely to describe the type of an interferometer, its optical layout or its physical dimensions. We propose to use the following definitions for describing the location, type and optical layout of interferometric detectors.

- *Geometry*: This describes the position information of one or several interferometers, defined by the number of interferometers, their location and relative orientation. The detector shown in Figure 1 is defined by the following geometry: three interferometers of equal arm length are located in a plane. The interferometer arms are aligned such that together they form an equilateral triangle.
- *Topology*: The topology describes the optical system formed by its core elements, examples are the classical Michelson, Sagnac and Mach-Zehnder topologies [25]. The triple Michelson illustrated in Figure 1 utilises the Michelson topology, even though it employs arm cavities and recycling techniques.
- *Configuration*: This describes the detail of the optical layout and the set of parameters that can be changed for a given topology, ranging from the specifications of the optical core elements to the control systems, including the operation point of the main interferometer. Also the addition of optical components to a given topology is often referred to as a change in configuration.

In order to reach their ambitious goals, third-generation detectors will very likely be located deep underground. First of all, this can significantly reduce seismic noise and gravity gradient noise (see [15, 16] for a review on gravity gradient noise and [17] for a comparison between the seismic noise at the underground and surface interferometers in Japan). Secondly, going underground might provide a relatively easy realization of (very tall) low frequency suspensions. Regardless of the details of the implementation, it is clear that a new infrastructure will allow us to design interferometers that are completely different from the single Michelson that characterises present laser-interferometric detectors. Hence the interferometer geometry and topology become an important area of research².

For the full extraction of astrophysical information, and in particular the source position in the sky (for short-lived signals as those from *e.g.* coalescing binaries and supernovae) a network of largely separated instruments is mandatory. The design and geometry of such a detector network is not the subject of this article. Instead we concentrate on the interferometer geometry at one detector site. In particular, we describe the benefits of using three Michelson interferometers in one location, using a triangular geometry.

The design of a third-generation interferometer will probably take place in two phases. During an initial phase the analysis of advantages and disadvantages of different geometries, topologies and configurations can be pursued independently. During the second phase, however, a system design, including all aspects of the interferometer, will be required. The remainder of the paper focuses on the first phase and investigates the merits of a triangular geometry; we will review some features of single and multiple Michelson interferometers to conclude that a triangular set of three Michelson interferometers in a plane combines the most interesting features.

² The ET design study proposal emphasises the option for an instrument based on a new topology.

3. Virtual Interferometry

The term *virtual interferometry* is used in the literature for describing various techniques. Most commonly it describes the use of numerical simulations to study the features of an interferometer [26] or techniques in astronomy where an interference between two measured optical signals is performed numerically as part of the data analysis process [27]. We propose to use the term with respect to interferometric gravitational-wave detectors for describing linear combinations of interferometer output signals that provide a readout equivalent to an additional optical interference.

The current literature on gravitational wave detection shows two very interesting and as yet unrelated methods of combining interferometer signals numerically for enhancing the sensitivity of a detector. The most prominent example is the technique of *time-delay interferometry* (TDI; see [28] for a review, and references therein), a technique developed primarily to suppress the otherwise overwhelming contribution from laser frequency noise in LISA. It creates the main detector output signals (also called observables in this context) by time shifting and linearly combining the many available interferometer output signals [29]. These observables can be understood as the output of ‘virtual’ interferometers. Examples are the two 60° pseudo-Michelson observables with uncorrelated noise [30] and a so-called *Sagnac* observable [31], in which the contribution from gravitational waves is largely suppressed at frequencies lower than the inverse of the round-trip light-time of photons along the arms of the instrument.

The second prominent application of numerical combinations of optical signals is called *displacement-noise free interferometry* [23, 32]. Even though it uses a very similar idea of combining interferometer signals that contain the gravitational wave signal with different phase information, the aim is slightly different. This method, so far exclusively aimed at ground-based detectors, can be used to discriminate gravitational radiation from signals that are generated by any other displacement of the main mirrors, for example, through seismic or thermal noise. The simple term ‘displacement noise’ covers many limiting noise sources of state-of-the-art detectors. Removing or reducing such noise would be equivalent to an improvement in sensitivity over a wide frequency range, which so far no other proposed technology can promise. The proposed displacement-noise-free methods are so far still proof-of-principle designs and far from any practical application. Moreover, their effective noise reduction is most effective at frequencies above $\sim c/L$ [32]. For ground-based detectors, of which even future detectors are likely to have arm lengths less than 30 km, this frequency region $f > 10$ kHz is typically not dominated by displacement noise but shotnoise. However, research into these technologies is on-going; the potential for increasing the detector sensitivity by a large factor and over a wide band makes displacement-noise reduction one of the most exciting ideas for future interferometers.

Both TDI and displacement-noise free interferometry utilise extra interferometer output channels to dramatically improve the performance of the respective instrument. Future detectors will probably make increasing use of such ‘virtual interferometry’. Regardless of the exact implementation, this requires multiple readout channels for the gravitational-wave signal, which can be achieved by using co-located interferometers or alternatively by implementing new interferometer configurations. Both methods have already been used to create so-called null-stream channels (see below).

4. Advantages of Multiple co-located Interferometers

4.1. Generation of Null-Streams

An important part of the data analysis for gravitational-wave detectors is the early identification of ‘false candidates’; noise events that could be mistaken for gravitational-wave signals. A powerful method, especially regarding unmodelled sources, is the construction of so-called *null-streams*. A null-stream is defined as a data stream formed by a linear combination of detector signals such that the gravitational-wave contribution exactly cancels (within the calibration accuracy), while signals of other origin are left with a finite amplitude. Therefore every event that can be detected in the null-stream as well as the standard detector output can be discarded as noise.

The GEO 600 detector employs a null-stream which is created from two output channels of the main interferometer, both of which carry the gravitational wave signals [34]. This type of null-stream is aimed mainly at identifying noise events that originate in the data acquisition system. In addition, it recognises disturbances inside the interferometer that have an optical transfer function different from gravitational-wave events. However, this particular type of null-stream technique cannot distinguish between gravitational waves and similar optical signals like those from displacements of the interferometer optics.

Null-streams in the context of burst analysis for a network of detectors were first investigated by Gürsel and Tinto [35]. More recently, this technique has received much attention and have been further developed [36, 37, 38] due to the availability of large data sets collected during science runs and the need to employ robust methods to discriminate between transient noise fluctuations and signals of astrophysical origin.

In general it is always possible to form a null-stream from three, not all co-aligned, detectors. The sensitivity of this stream to noise events does however depend strongly on the relative instrument rotation. A general formalism to construct null-streams was developed in [37] and this technique is used in a number of on-going searches. If the instruments are aligned, two interferometers allow us to synthesise an observable which is insensitive to gravitational waves [37]. The simplest null-stream can be created in real time from a pair of redundant detectors as done at LIGO-Hanford [36]: Two co-aligned Michelson interferometers have been installed on the same site so that the null-stream that cancels gravitational waves of all kinds at all times can be computed by simply taking the difference of the detector signals:

$$h_{\text{null}} = h_1 - h_2, \quad (1)$$

where h_i stands for the main detector channel calibrated in gravitational-wave strain.

An equally simple and powerful null-stream can be obtained using three Michelson interferometers located in a plane. Using the framework developed in [38, 39] it can be shown that three Michelson interferometers orientated at 0° , 30° and 60° (see Figure 2D) represent a fully redundant set such that the output signal of each individual interferometer can be simply generated from the respective other two without undue amplification of the detector noise. In particular, for three Michelson interferometers oriented at 0° , 120° and 240° , one obtains:

$$-h_{0^\circ} = h_{240^\circ} + h_{120^\circ}, \quad (2)$$

where the sign of the operation is defined by which ports of the Michelson interferometers are used to inject the laser light (see Appendix A for a brief derivation

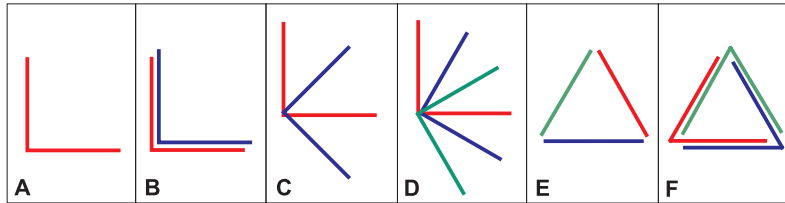


Figure 2. A comparison of several geometries for future ground-based detectors: **A:** A simple Michelson interferometer is sensitive only to a linear combination of the two polarisation amplitudes. **B:** Two co-aligned Michelson interferometers provide redundancy and the possibility to generate a null-stream (and as for case A are sensitive only to a linear combination of the two polarisation amplitudes). **C:** Two Michelson interferometers rotated 45° with respect to each other can fully resolve both polarisation amplitudes. **D:** Three rotated Michelson interferometers provide redundancy and the possibility to generate a null-stream. They also can measure both polarisations (the geometries shown as C and D feature intersection tubes. Similar geometries in which the Michelson interferometers do not overlap might be more practical, depending on the properties of the detector site, see [14]). **E:** A LISA-like triangular configuration, in which the interferometer arms are single cavities and there is no optical recombination. **F:** A Triple Michelson interferometer configuration consisting of three individual Michelson interferometers.

of this relation). It follows that using this detector geometry a null-stream can again be created by a simple addition of the three main interferometer outputs.

This shows that a detector composed of three Michelson interferometers, which are rotated by 30° or 120° with respect to each other, features redundancy and null-stream capabilities like those of co-linear Michelson interferometers. Furthermore, this set of three Michelson interferometers provides redundancy to maintain full sensitivity to *both* gravitational wave polarisations, see next section.

4.2. Sensitivity to the Gravitational-Wave Polarisation

A Michelson interferometer provides maximal sensitivity to a specific polarisation (or, equivalently measures only a linear combination of the two polarisation amplitudes). Two interferometers rotated by 45° as shown in Figure 2C allow full reconstruction of both polarisation amplitudes. Generally, gravitational waves will not arrive at the detector in the optimal polarisation for one interferometer, thus the detection of the second polarisation increases the total signal strength (see Figure 3). Furthermore, two such oriented Michelson interferometers can be used to detect both polarisations and to determine the polarisation angle. This is important to fully resolve the geometry of a source and test general relativity [40].

It is straightforward to show that three Michelson interferometers, which are rotated with respect to each other in an appropriate way, can also measure the polarisation of the gravitational wave. By the same analysis as for the null-stream construction it can be shown that we can synthesise the output signal of a ‘virtual’ Michelson³ at 45° from two otherwise equal interferometers rotated by 120° and 240° :

$$h_{45^\circ} = \frac{1}{\sqrt{3}}(h_{240^\circ} - h_{120^\circ}) \quad (3)$$

³ Note that this is equivalent to the well-know result derived for the LISA detector [30].

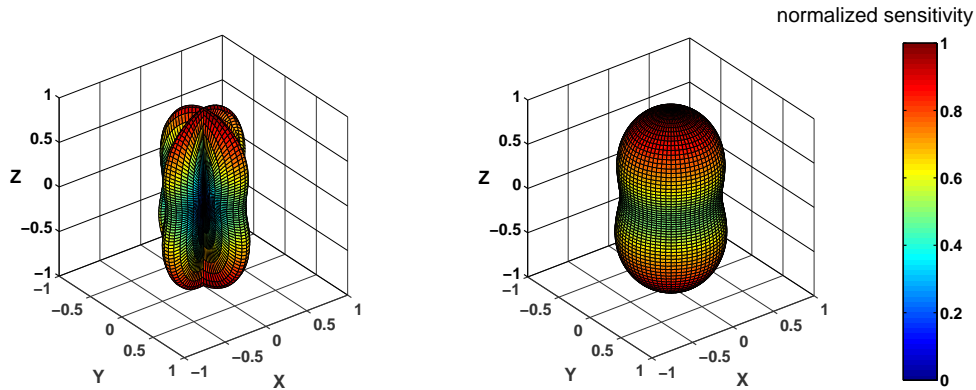


Figure 3. The response of a detector to a linear polarised gravitational wave as a function of the detector orientation. Both plots show the normalised sensitivity to a wave travelling along the z-axis. Each data point represents the sensitivity of the detector for a specific detector orientation defined by the detector normal passing the respective data point and the origin. The colour of the data point as well as its distance from the origin indicate the magnitude of the sensitivity. The left plot depicts the response of a single Michelson, while the right plot gives the response of a set of three Michelson interferometers in a triangular geometry as shown in Figure 2 F.

Therefore the set of three Michelson interferometers offers the same advantages with respect to gravitational wave polarisation as two interferometers that are oriented by 45° to each other.

So far we have used the term redundancy as an equivalent to null-stream generation. However, we should consider redundancy also under operational aspects. The fact that we reconstruct a third Michelson interferometer from two other means that we can perform hardware upgrades or maintenance sequentially on the entire detector without interrupting data taking. In fact, with one Michelson not operating we would still be able to fully detect both gravitational wave polarisations, and only the construction of a null-stream would become impossible. The possibility of having a duty cycle as close as possible to 100% for the gravitational wave data channels becomes an important asset, especially when we consider each detector to be part of a larger network.

5. Interferometer Topologies

To date no laser interferometer topology other than the Michelson has been used for gravitational wave detection. However, some very advanced noise reduction techniques proposed for future detectors are based on topologies of the Sagnac interferometer, the Fox-Smith cavity or the Mach-Zehnder interferometer [21, 22, 23].

It is worth noting that a triangular geometry as discussed above is conceivable with different interferometer topologies. In particular it is possible to use different topologies while maintaining the L-shape of the single interferometers as displayed in figure 4. Therefore, for example, three Sagnac interferometers or three cavities could be used to form a triangle. Such detector designs can provide similar benefits as described above for the triple Michelson geometry so that the triangular geometry is largely independent of the topology of the individual interferometers.

The case for alternative topologies is largely based on ideas for the reduction of quantum noise. In general, the signal-to-noise ratio of a single interferometer is different for each topology, with the actual difference depending also on the type of noise under investigation. However, it is not possible to identify a topology with a meaningful signal-to-noise ratio or sensitivity since these vary dramatically with the interferometer *configuration*. Consequently, detailed interferometer designs must be studied for comparing different topologies. To-date such effort has only been fully undertaken for the Michelson topology including ongoing research which shows that the Michelson topology offers interesting possibilities for new quantum noise reduction techniques [18].

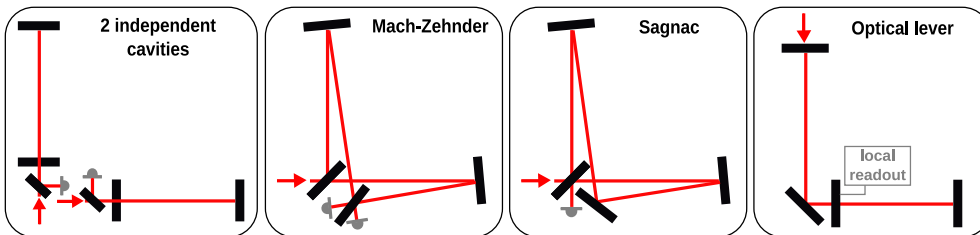


Figure 4. Four example interferometer topologies that can be used in a L-shaped form: 1) two single cavities 2) Mach-Zehnder interferometer 3) Sagnac interferometer 4) Optical lever.

During the design and construction of the first generation of detectors the Sagnac topology has been investigated and prototypes have been build [19] but eventually it did not show significant advantages over the Michelson topology [20]. More recently it has been proposed to use the Sagnac topology as a *speed meter* [21] to reduce the quantum noise. The Sagnac topology can be hosted in different ways in a triangular geometry: each Sagnac as an equilateral triangle, or as an L-shaped zero-area Sagnac. Noise couplings due to the Sagnac effect favor the zero-area Sagnac topology: it can be shown that for a typical choice of optical parameters this extra noise couplings do not impose stringent new requirements in the case of a zero-area Sagnac interferometer, see Appendix C.

A detailed study of the proposed alternative topologies will be a core activity of the ET design study and is beyond the scope of this paper. We note that Michelson-based detectors currently offer the advantage of using the experience as well as the advanced optical technologies of the first two detector generations and thus at least must be taken as a reference against which other topologies must be compared.

6. Triple Michelson Interferometer

A triangular detector geometry as displayed in Figure 2F has been proposed already in 1985 by Rüdiger, Winkler and collaborators [13, 14]. Henceforth we will call this layout a *triple Michelson* to differentiate this geometry from other triangular ones.

It is useful to consider whether a triangular configuration would allow us to reconstruct completely the geometry of an arbitrary gravitational wave source. For simplicity we consider the case of a (non-spinning) binary system, but the counting argument that we present here equally applies to other burst signals (it is not appropriate however for stochastic signals or long-lived signals, such as those from

rotating neutron stars). In order to reconstruct the geometry of a source one needs to estimate (at least) five parameters: the luminosity distance to the source, two angles that identify the source position in the sky, and two angles that describe the orientation of the orbital angular momentum (one usually uses the polarisation angle ψ and the inclination angle ι). A single Michelson interferometer would provide only two independent quantities, and the problem would be severely underdetermined. A triangular topology, on the other hand would provide *four* independent constraints to measure five unknowns. An additional interferometer in a different location would therefore be still necessary to fully break the degeneracy, which is however much less severe than in the case of a single Michelson.

The triangular geometry is equivalent to the one in Figure 2D, with the only difference⁴ that the 60° opening angle of the interferometers reduces the strain sensitivity to $\sin(60^\circ) = 0.87$ of the optimal one. Such a moderate loss of sensitivity is compensated by a substantial reduction in the required underground space: compared with the geometry depicted in Figure 2D, a triangular detector only requires half the tunnel length and only 3 instead of 7 end stations. It can also be shown that the sensitivity of the triple Michelson is very similar to a set of four right-angled Michelson detectors oriented at 0° and 45° , see Appendix B. Such a configuration is optimal in the sense of providing the whole number of independent observables that can be obtained by an *arbitrary* number of co-planar and co-located instruments. In fact, the addition of more instruments in the same location and plane would not change the number of independent information that can be obtained, as one would be able to reconstruct the output of this additional instrument as a linear combination of the readouts of the two Michelsons given by the triangular topology. The triple Michelson can be considered the minimal (in terms of enclosed area and number of end stations) detector geometry that combines all features of the various options using co-located, co-planar Michelson interferometers.

7. Summary and Outlook

The Michelson interferometer is ideally suited for measuring gravitational waves. It combines large bandwidth with good sensitivity to gravitational wave strain. Second-generation gravitational wave detectors are based on modern Michelson interferometers enhanced by advanced techniques, like power- and signal recycling. It is expected that such detectors will beat the Standard Quantum Limit of interferometry in a small frequency range. [41, 42].

Third-generation instruments might be constructed at new detector sites and therefore new interferometer layouts can be considered. In this paper we have outlined the concept of detector *geometry*, *topology* and *configuration* for investigating possible designs for third-generation detectors. We have further evaluated the idea of three co-located interferometers in a triangular geometry. The original proposal of this geometry was motivated mainly by the idea that such a detector had the ability to detect both gravitational wave polarisations. In this article we have shown that such a geometry offers significant advantages based on ‘virtual interferometry’ techniques. In particular, we have highlighted the fact that the interferometer set is fully redundant and offers the possibility to create an efficient null-stream from the local detector data.

⁴ The three Michelsons are not exactly co-located, for 10 km long arms the interferometer signals can be subject to a time delay up to the order of $L/c \approx 0.3$ ms.

Several known interferometer topologies can be employed in the triangular geometry and such topologies have to be re-evaluated in the light of the demanding sensitivity of third-generation detectors.

As part of the European design study 'Einstein gravitational-wave Telescope' a careful and in-depth system design will begin with the aim of understanding which detector geometry and topology is optimal for third-generation detectors. The triple Michelson detector presents a realistic concept as it combines a well tested and well understood interferometer design with new possibilities, mainly based on the combination of multiple interferometric signals. These advantages will play a strong role in deploying gravitational-wave *telescopes* capable of continuous surveys. Therefore this detector geometry should be considered as a meaningful starting point for design studies that are about to begin.

8. Acknowledgement

We would like to thank Albrecht Rüdiger, Roland Schilling and Harald Lück for many useful discussions. We are particularly grateful to Albrecht Rüdiger for providing us with the original proposal of the triple Michelson detector. This work has been supported by the Science and Technology Facilities Council (STFC) and the European Gravitational Observatory (EGO). This document has been assigned the LIGO Laboratory document number LIGO-P080019-00-Z.

Appendix A. Virtual Michelsons

From [39] we obtain the following general expression for the response function of a Michelson interferometer to gravitational waves:

$$h(t) = F_+(t)h_+(t) + F_\times(t)h_\times(t) \quad (\text{A.1})$$

where F_+ and F_\times are the beam pattern function which in turn can be written as:

$$\begin{aligned} F_+(t) &= \sin \zeta (a(t) \cos 2\psi + b(t) \sin 2\psi) \\ F_\times(t) &= \sin \zeta (b(t) \cos 2\psi - a(t) \sin 2\psi) \end{aligned} \quad (\text{A.2})$$

with ζ the opening angle of the interferometer arms and ψ the polarisation angle of the gravitational wave. $a(t)$, $b(t)$ are complex functions of the detector location in space and time. We are only interested in their dependence on the detector rotation around its normal, here described by the angle γ . We can thus simplify a , b to:

$$\begin{aligned} a(\gamma) &= C_1 \sin 2\gamma + C_2 \cos 2\gamma \\ b(\gamma) &= C_3 \sin 2\gamma + C_4 \cos 2\gamma \end{aligned} \quad (\text{A.3})$$

with C_n as functions of time as well as the remaining parameters specifying the position of the detector and the location of the gravitational wave source. In the following we arbitrarily set the polarisation angle to $\psi = 0$. This yields:

$$\begin{aligned} h(\gamma) &= \sin \zeta [(C_1 \sin 2\gamma + C_2 \cos 2\gamma) h_+ \\ &\quad + (C_3 \sin 2\gamma + C_4 \cos 2\gamma) h_\times] \end{aligned} \quad (\text{A.4})$$

In particular we obtain:

$$\begin{aligned} h(0^\circ) &= \sin \zeta [C_2 h_+ + C_4 h_\times] \\ h(45^\circ) &= \sin \zeta [C_1 h_+ + C_3 h_\times] \end{aligned} \quad (\text{A.5})$$

Using simple addition and subtraction rules for sin and cos we can further write:

$$\begin{aligned} h(120^\circ) + h(240^\circ) &= -\sin \zeta [C_2 h_+ + C_4 h_\times] = -h(0^\circ) \\ h(120^\circ) - h(240^\circ) &= -\sqrt{3} \sin \zeta [C_1 h_+ + C_3 h_\times] = -\sqrt{3} h(45^\circ) \end{aligned} \quad (\text{A.6})$$

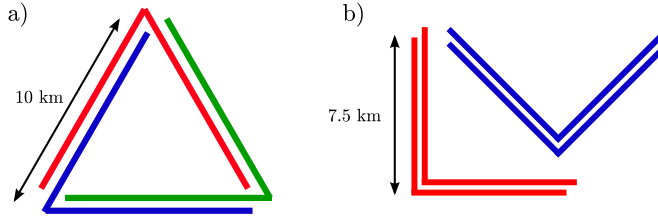


Figure B1. Comparison of two detector geometries that utilise exactly the same tunnel length and feature almost exactly the same sensitivity, see text. The left sketch a) shows three uncorrelated Michelson interferometers in a triangular tunnel system. On the right b) four uncorrelated Michelson interferometers are located in two L-shaped tunnel systems. In both cases the total tunnel lengths is 30 km and each tunnel segment hosts two interferometer arms, preferably in separate vacuum systems.

Appendix B. Triangle versus right angled interferometers

We want to compare the sensitivity of a triangular detector to that of a similar detector that uses right-angled Michelsons. In order to do so we assume the following constraints: both detectors should have the same total tunnel length and the same number of laser beams in each tunnel segment. The two best detector geometries within these constraints are shown in figure B1. In addition, we consider all interferometers of one detector to be uncorrelated (probably housed in separate vacuum systems).

It is useful for this example to relate the SNR of any given detector to a reference instrument, here, a single Michelson interferometer with orthogonal arms of 10 km length. The signal strength of the triangular setup shown in figure B1 can be compared to the reference detector by combining the three interferometer signal. For $\gamma = 0^\circ$ we obtain:

$$h_{\Delta}(0^\circ) = h(0^\circ) - h(120^\circ) - h(240^\circ) = 2h(0^\circ) \quad (\text{B.1})$$

With h_{Δ} the signal output of the triangular detector. We can then approximate:

$$\frac{\text{SNR}_{\Delta, L=10 \text{ km}}}{\text{SNR}_{\text{MI}, L=10 \text{ km}}} = \frac{2}{\sqrt{3}} \sin(60^\circ) = 1 \quad (\text{B.2})$$

And for $\gamma = 45^\circ$ we obtain:

$$\frac{\text{SNR}_{\Delta, L=10 \text{ km}}}{\text{SNR}_{\text{MI}, L=10 \text{ km}}} = \frac{\sqrt{3}}{\sqrt{2}} \sin(60^\circ) \approx 1.06 \quad (\text{B.3})$$

Similarly we can compute the SNR of the right-angled setup b) by adding the signals of two parallel interferometers (oriented either at 0° or 45°):

$$\frac{\text{SNR}_{\text{two MI}, L=7.5 \text{ km}}}{\text{SNR}_{\text{MI}, L=10 \text{ km}}} = \frac{2}{\sqrt{2}} \frac{7.5}{10} \approx 1.06 \quad (\text{B.4})$$

This shows that the triangle geometry has in the worst case a 6% lower sensitivity. However, in practice, the sensitivity of the right-angled detector might be worse since the condition of uncorrelated noise will be much more difficult to achieve because always two interferometers share exactly the same location.

Appendix C. The Sagnac effect

One of the prime uses of the Sagnac interferometer is to measure rotation, via the *Sagnac effect* [24]: In an otherwise undisturbed Sagnac interferometer the relative phase of the beams interfering at the beam splitter is proportional to the effective enclosed area A , the angular frequency Ω of the interferometer rotation and the angular frequency of the light ω :

$$\phi = \frac{4A}{c^2} \Omega \omega \quad (\text{C.1})$$

Thus the Sagnac effect must be evaluated as a possible channel for coupling laser frequency noise or seismic noise into the gravitational wave channel. To minimise the effect the interferometer should be designed as a zero-area Sagnac. However, small misalignments of the optical beams will cause A to be non-zero, as indicated in figure C1. In the following we present noise estimations for an example Sagnac layout with 10 km arm length.

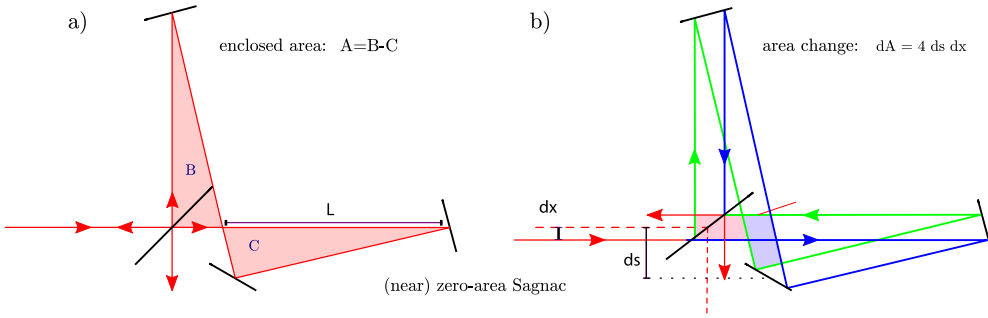


Figure C1. a) Zero-area Sagnac interferometer: by carefully adjusting the arm length and the angle of the end mirrors the enclosed areas B and C are made equal such that the effective enclosed area A is zero. b) Area change due to transverse beam displacement: in practice a small change of the beam position, or the interferometer alignment will cause the enclosed area to change, so that A is not zero on average and also fluctuating at higher frequencies.

At first we consider the Sagnac effect due to the Earth's rotation. We have arbitrarily chosen the latitude of Strasbourg and assume a constant rotation frequency of $\Omega_S = \Omega \sin(48^\circ 33')$, where Ω is the rotational frequency of the Earth. Any change in the enclosed area A or the laser frequency ν will couple into the optical phase. The latter can be interpreted as a new coupling mechanism for frequency noise with the coupling given by the projection of the detector sensitivity to frequency noise:

$$\Delta\nu = \frac{L c^2}{A \Omega_S \lambda \cos(\alpha)} \cdot h \approx \frac{L c^2}{A \Omega_S \lambda} \cdot h \quad \text{for small } \alpha \quad (\text{C.2})$$

In order to estimate the enclosed area A we assume an average miscentering or misalignment of the beams to be of the order of 0.1 mm which corresponds to $A \approx 0.5 \cdot 10 \text{ km} \cdot 0.1 \text{ mm} = 0.5 \text{ m}^2$. For an example sensitivity of $h = 6 \cdot 10^{-24} \sqrt{\text{Hz}}$, which represents the target sensitivity of the Einstein Telescope at 10 Hz, we can thus estimate the frequency noise requirement to be:

$$\Delta\nu \lesssim 1.9 \cdot 10^8 \frac{\text{Hz}}{\sqrt{\text{Hz}}} \left(\frac{h \sqrt{\text{Hz}}}{6 \cdot 10^{-24}} \right) \left(\frac{L}{10 \text{ km}} \right) \left(\frac{0.5 \text{ m}^2}{A} \right) \left(\frac{5 \cdot 10^{-5} \text{ Hz}}{\Omega_S} \right) \left(\frac{1064 \text{ nm}}{\lambda} \right) \quad (\text{C.3})$$

which does not cause any concern. We must also consider the coupling of seismic noise, via two different effects. First of all, the seismic disturbances of the interferometer as a whole includes a rotational component which can be characterised by replacing Ω_S by an dynamic term in equation C.1. To estimate the effect we have assumed the simplest case in which the seismic noise at the corners of the triangle is uncorrelated and we can write the spectral density of the rotation angle as:

$$\Delta\Omega_\sigma = \arctan\left(\frac{\Delta\sigma}{L}\right) \quad (\text{C.4})$$

with $\Delta\sigma$ the amplitude spectral density of the seismic disturbances. We can further project the detector sensitivity to the seismic noise level using:

$$\Delta\sigma = L \tan\left(\frac{Lc}{A \cos(\alpha)} \cdot h\right) \quad (\text{C.5})$$

and again we assume $\alpha \ll 1$ to compute a requirement for the seismic noise:

$$\Delta\sigma \lesssim 1.8 \cdot 10^{-7} \text{m} \left(\frac{h \sqrt{\text{Hz}}}{6 \cdot 10^{-24}}\right) \left(\frac{L}{10 \text{ km}}\right) \left(\frac{0.5 \text{ m}^2}{A}\right) \quad (\text{C.6})$$

Another way in which the seismic noise can couple into optical phase noise is through misalignment of the optics or input beam jitter. Input beam jitter can be interpreted as a change of the enclosed area as shown in figure C1. The noise projection factor is given by:

$$\Delta x = \frac{Lc}{4\Omega_S \cdot ds \cos(\alpha)} \cdot h \quad (\text{C.7})$$

with ds being the distance between the beam splitter and the central turning mirror as shown in figure C1. This leads to the following requirement for input beam jitter:

$$\Delta x \lesssim 8.3 \cdot 10^{-8} \text{m} \left(\frac{h \sqrt{\text{Hz}}}{6 \cdot 10^{-24}}\right) \left(\frac{L}{10 \text{ km}}\right) \left(\frac{5 \cdot 10^{-5} \text{ Hz}}{\Omega_S}\right) \left(\frac{1 \text{ m}}{ds}\right) \quad (\text{C.8})$$

Such a requirement is well within the performance of the existing mode cleaner systems of current detectors. In summary, the noise introduced by the Sagnac effect is negligible provided that the interferometer is designed as a zero-area Sagnac and that the beam alignment can be performed accurately enough to ensure a small effective enclosed area.

References

- [1] Hild S *et al* 2006 The Status of GEO 600 *Class. Quantum Grav.* **23** S643–651
- [2] Acernese F *et al* 2004 Status of VIRGO *Class. Quantum Grav.* **21** S385–94
- [3] Sigg D *et al* 2004 Commissioning of LIGO detectors *Class. Quantum Grav.* **21** S409–15
- [4] Takahashi R 2004 Status of TAMA300 *Class. Quantum Grav.* **21** S403–8
- [5] P. Fritschel 2003 in Gravitational Wave Detection, edited by M. Cruise and P. Saulson, Proc. SPIE 4856, 282291.
- [6] <http://wwwcascina.virgo.infn.it/advirgo/>
- [7] Kuroda K *et al* 2006 The status of LCGT *Class. Quantum Grav.* **23** S215–21
- [8] Willke B *et al* 2006 The GEO-HF project *Class. Quantum Grav.* **23** S207–14
- [9] Lück H *et al* 2007 Plans for E.T. (Einstein Telescope), A European 3rd generation gravitational wave observatory, presented at the AMALDI 7 conference, Sydney
- [10] Einstein gravitational-wave Telescope 2007 Design study proposal submitted to European Union. Framework 7, INFRA-2007-2.1-01, Design studies for research infrastructures in all S&T fields
- [11] Hild S *et al* 2008 Pushing towards the ET sensitivity using 'conventional' technology *arXiv:0810.0604v2 [gr-qc]*

- [12] LISA, Laser Interferometer Space Antenna, <http://lisa.jpl.nasa.gov>
- [13] Winkler W *et al* 1985 Plans for a large gravitational wave antenna in Germany, MPQ report 101 (presented by A Rüdiger at the 4th Marcel Grossmann Meeting, Rome 1985)
- [14] Maischberger K *et al* 1985 Vorschlag zum Bau eines großen Laser-Interferometers zur Messung von Gravitationswellen, MPQ report 96 (in German)
- [15] Hughes S A and Thorne K S 1998 Seismic gravity-gradient noise in interferometric gravitational-wave detectors *Phys. Rev. D* **58** 122002
- [16] Thorne K S and Winstein C J 1999 Human gravity-gradient noise in interferometric gravitational-wave detectors *Phys. Rev. D* **60** 082001
- [17] Ohashi M *et al* 2003 Design and construction status of CLIO *Class. Quantum Grav.* **20** 599
- [18] Rehbein H and Müller-Ebhardt H *et al* 2008 Double optical spring enhancement for gravitational-wave detectors *Phys. Rev. D* **78** 062003
- [19] Sun K.-X and Fejer M. M *et al* 1996 Sagnac Interferometer for Gravitational-Wave Detection *Phys. Rev. Lett.* **76** 3053–3056
- [20] Mizuno J *et al* 1997 Frequency response of Michelson- and Sagnac-based interferometers *Optics Communications* **138** 383 - 393
- [21] Chen Y 2003 Sagnac interferometer as a speed-meter-type, quantum-nondemolition gravitational-wave detector *Phys. Rev. D* **67** 122004
- [22] Danilishin S. L and Khalili F. Y 2006 Practical design of the optical lever intracavity topology of gravitational-wave detectors *Phys. Rev. D* **73** 022002
- [23] Chen Y *et al* 2006 Interferometers for Displacement-Noise-Free Gravitational-Wave Detection *Phys. Rev. Lett.* **97** 151103
- [24] Malykin G. B 2000 The Sagnac effect: correct and incorrect explanations *Physics-Uspokhi* **43** 1229-1252
- [25] Hecht E 2002 Optics *Addison-Wesley* 4th edition
- [26] Brilliet A *et al* 2003 Virtual gravitational wave interferometers with actual mirrors *Phys. Rev. D* **67** 102006
- [27] Cai L Z *et al* 2006 Virtual shearing interferometry by digital holography *Optics Communications* **259** 64–69
- [28] Dhurandhar S V and Tinto M 2005 Time-delay interferometry, *Living Reviews in Relativity*, **8** 4
- [29] Nayak K R and Vinet J-Y 2004 Algebraic approach to time-delay data analysis for orbiting LISA *Phys. Rev. D* **70** 102003
- [30] Cutler C 1998 Angular resolution of the LISA gravitational wave detector *Phys. Rev. D* **57** 12
- [31] Tinto M *et al* 2001, *Phys. Rev. D* **63** 021101
- [32] Chen Y and Kawamura S 2006 Displacement- and Timing-Noise Free Gravitational-Wave Detection *Phys. Rev. Lett.* **96** 231102
- [33] Andersson N and Kokkotas K D, 1998 Towards gravitational wave asteroseismology, *MNRAS*, **299**, 1059
- [34] Hewitson M and Ajith P 2005 Using the null-stream of GEO 600 to veto transient events in the detector output *Class. Quantum Grav.* **22** S4903–4912
- [35] Gürsel Y and Tinto M 1989 Near optimal solution to the inverse problem for gravitational-wave bursts *Phys. Rev. D* **40** 3884
- [36] Ajith P *et al* 2006 Null-stream veto for two co-located detectors: implementation issues *Class. Quantum Grav.* **23** S741–749
- [37] Chatterji S *et al* 2006 Coherent network analysis technique for discriminating gravitational-wave bursts from instrumental noise *Phys. Rev. D* **74**
- [38] Wen L and Schutz B 2005 Coherent network detection of gravitational waves: the redundancy veto *Class. Quantum Grav.* **18** S1321–35
- [39] Jaranowski P *et al* 1998 Data analysis of gravitational-wave signals from spinning neutron stars: The signal and its detection *Phys. Rev. D* **58** 063001
- [40] Will, C M 2006, The Confrontation between General Relativity and Experiment, *Living Reviews in Relativity*, **9**, 3
- [41] Buonanno A and Chen Y 2001 Quantum noise in second generation, signal-recycled laser interferometric gravitational-wave detectors *Phys. Rev. D* **64** 042006
- [42] Chelkowski S *et al* 2007 Coherent control of broadband vacuum squeezing *Phys. Rev. A* **75** 043814